Proceedings of the 17th World Congress
The International Federation of Automatic Control
Seoul, Korea, July 6-11, 2008

Obstacle Avoidance for Wheeled Robots in Unknown Environments using Model Predictive Control ⋆

Yongsoon Yoon * , **Tokson Choe** ** , **Yongwoon Park** ** **and H. Jin Kim** ***

* *Continental Automotive System, Icheon, Korea (Tel: +82-31-645-4758; yongsoon.yoon@continental-corporation.com)*
** *Agency for Defense Development, Daejon, Korea (e-mail: tschoe@add.re.kr, woon5901@hanafos.com)*
*** *School of Mech. & Aero. Eng. Seoul National Univ., Seoul, Korea (Tel: +82-2-880-7392; email: hjinkim@snu.ac.kr)*

Abstract: This paper presents a model predictive approach for obstacle avoidance of car-like unmanned ground vehicles (UGVs). An optimal tracking problem while avoiding obstacles in unknown environments is formulated in terms of cost minimization under constraints. Information on obstacles can be incorporated online in the nonlinear model predictive framework and kinematic constraints are treated by Karush-Kuhn-Tucker (KKT) condition. The overall problem is solved real-time with nonlinear programming. This approach is applied to car-like robots including tire models while explicitly considering the dimension of the UGV rather than treating it as a dimensionless cart model. Two kinds of potential-like terms are employed in the cost function for obstacles avoidance. The first term is to consider the distance between the UGV and the obstacle, and the second one is to consider the parallax information of the UGV about the obstacles. Simulation results show that both two approaches can make safe steering in a simple environment, but in a complex environment such as an urban area, the approach based on the modified parallax (MP) was more successful in the view of the computation time and safe steering.

1. INTRODUCTION

UGVs are employed in various military, reconnaissance and materials handling applications. Often UGVs are commanded to perform pre-defined maneuvers or to follow a pre-planned path designated by an off-line mission-level planning algorithm. But many of these applications require a UGV to move in unknown environments with dynamic and physical constraints.

In this paper, we present a model predictive method for active steering control of a UGV based on successive on-line optimization of the nonholonomic UGV dynamics. In order to use this approach as a local obstacle avoidance planner for the UGV shown in Fig. 1, we use a bicycle model to predict the future evolution of the system.

Many local obstacle avoidance schemes use purely reactive methods based on sensor inputs (Rimon et al [1992], Fox et al [1997], Simmon [1996], Minguez et al [2000]). Some take into account the dynamics and kinematics constraints (Ulrich et al [2000]). These approaches are computationally efficient, but the vehicle can get stuck in local minima, sometimes the discretization of the world

⋆ This work was supported by the Korea Science and Engineering Foundation (KOSEF) grant funded by the Korea government (MOST) (No. R0A-2007-000-10017-0), and by the Agency for Defense Development under the award 0498-20070019, administered via the Institute of Advanced Aerospace Technology at Seoul National University, Korea.

Fig. 1. UGV in consideration, its mass, momentum of inertia, length and width are 807 kg, 429.649 kgm^2, 2.150 m, and 1.290 m, respectively.

is required, or the full dynamics cannot be incorporated. In Arras et al [2002], the dimension of the vehicle was considered with a reduced dynamic window. But at high speed, this approach is not easy for applications.

Recently, predictive active steering control for autonomous vehicle systems was studied (Borrelli et al [2005], Falcone et al [2007]), with a tire model (Bakker et al [1987]). In these work, the autonomous vehicle was directed to follow the given reference which is assumed to be collision-free and achievable. In the case of unknown environments, it is difficult to acquire such a safe pre-defined reference. And the dimension of the vehicle is not considered. If the environments are complex and narrow, like an urban

environment, the dimension of the vehicle becomes very critical.

This paper considers the on-line obstacles avoidance as well as navigation toward the destination. If the vehicle runs into an unknown environment on the way to target point, controller predicts a future path and solves an optimization problem to plan collision-free trajectories toward the destination. Nonlinear model predictive control has been used to generate safe trajectories for unmanned aerial vehicles (Kim et al [2002]), but without considering the dimension of the vehicle, and at a lower sampling rate. In the current paper, both the critical safe distance from the obstacles and the critical modified parallax of the vehicle corresponding to the speed of the polygonal UGV are considered, which improves the performance while reducing the computation time.

2. VEHICLE MODEL

We use a bicycle model which has the yaw degrees of freedom, in combination with a tire model, to describe the UGV dynamics.

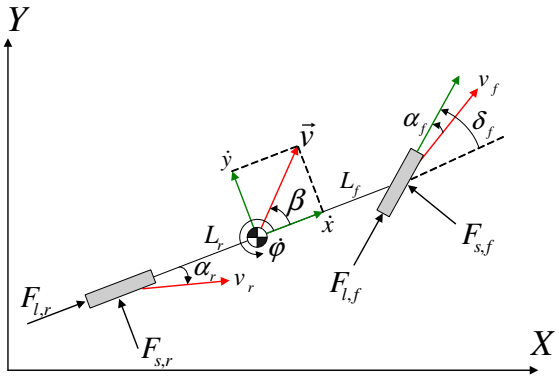

Fig. 2. A schematic diagram of the bicycle model.

We will use the following notation throughout this paper:

$(\cdot)_f$	front wheel
$(\cdot)_r$	rear wheel
$(\cdot)_x$	x-axis of the vehicle's body coordinate
$(\cdot)_y$	y-axis of the vehicle's body coordinate
$(\cdot)_s$	side direction
$(\cdot)_l$	longitudinal direction
$(\cdot)_k$	time step
$(\cdot)_{ref}$	reference tracking signals

This nomenclature refers to the robot model depicted in Fig. 2. v is the velocity vector of the center of gravity of the vehicle with respect to the vehicle's frame. α and β denote the slip angle of tires and the vehicle, respectively, defined as the angle between the velocity vector and their longitudinal axes. δ is the steering angle of a tire and ψ denotes the attitude of the vehicle with respect to the inertial frame. L_f and L_r denote the distance from the front axle to the center of gravity of the vehicle and from the rear axle to the center of gravity of the vehicle. In this paper, we consider front-wheel steering vehicle.

2.1 UGVs model

For the UGVs model, motion of the vehicle will be a function of the forces F_x, F_y and momentum M_z exerted on the center of gravity of the UGV (Wollherr [2002]). Equation (1) describes dynamics of the robot, where m is the mass of the robot.

$$\begin{aligned} mv(\dot{\beta}+\dot{\psi}) &= -F_x \sin\beta + F_y \cos\beta, \\ m\dot{v} &= F_x \cos\beta + F_y \sin\beta, \\ I_{zz}\ddot{\psi} &= M_z \end{aligned} \tag{1}$$

Setting up the equilibrium of forces and momentum yields (2), where $F_{sf}, F_{sr}, F_{lf}, F_{lr}$ are side and longitudinal tire forces exerted on each tire.

$$\begin{bmatrix} F_x \\ F_y \\ M_z \end{bmatrix} = \begin{bmatrix} -\sin\delta & 0 \\ \cos\delta & 1 \\ L_f\cos\delta & L_r \end{bmatrix} \begin{bmatrix} F_{sf} \\ F_{sr} \end{bmatrix} + \begin{bmatrix} \cos\delta & 1 \\ \sin\delta & 0 \\ L_f\sin\delta & 0 \end{bmatrix} \begin{bmatrix} F_{lf} \\ F_{lr} \end{bmatrix} \tag{2}$$

Tire forces (detailed in Bakker et al [1987]) for each tire are given by

$$F_l = f_l(\alpha, s, \mu, F_z)\ ,\ F_s = f_s(\alpha, s, \mu, F_z) \tag{3}$$

where s is the slip ratio defined as

$$s = \begin{cases} \dfrac{rw}{v_l} - 1\ , & \text{if } v_l > rw,\ \ v \neq 0 \ \text{ for breaking}\ , \\ 1 - \dfrac{v_l}{rw}\ , & \text{if } v_l < rw,\ \ w \neq 0 \ \text{ for driving}\ . \end{cases} \tag{4}$$

where, v_l is the longitudinal velocity of the tire. And the tire slip angles α_f, α_r are the function of β , $\dot{\psi}$, v as (5):

$$\begin{aligned} \alpha_f &= \delta_f - \tan^{-1}\left(\frac{v\sin\beta + L_f\dot{\psi}}{v\cos\beta}\right), \\ \alpha_r &= -\tan^{-1}\left(\frac{v\sin\beta - L_r\dot{\psi}}{v\cos\beta}\right). \end{aligned} \tag{5}$$

The parameter μ in (3) represents the road friction coefficient and F_z is the total vertical load of the vehicle. The vehicle's equations of motion in the inertial frame are

$$\begin{aligned} \dot{X} &= v\ \cos\beta\ \cos\psi\ -\ v\ \sin\beta\ \sin\psi, \\ \dot{Y} &= v\ \cos\beta\ \sin\psi\ +\ v\ \sin\beta\ \cos\psi. \end{aligned} \tag{6}$$

3. MODEL PREDICTIVE CONTROL PROBLEM

Since model predictive algorithm is solved in a discrete time domain, the system dynamics are discretized as (7)(Kim et al [2002]),

$$\begin{aligned} \xi(k+1) &= f_{s,\mu}^{dt}(\xi(k), u(k))\ , \\ \eta(k+1) &= h(\eta(k))\ . \end{aligned} \tag{7}$$

where the state variables and input are $\xi = [\ \beta\ \psi\ \dot{\psi}\ X\ Y\ ]^T$ and $u = \delta_f$ respectively, and the output vector is $\eta = [\ X\ Y\ ]^T$

3.1 Optimization algorithm

Equation (8) is the cost function, with the additional constraint terms on physical limits and penalty function for collision-free planning.

$$J = \phi(\tilde{\eta}_N) + \sum_{k=0}^{N-1} \Big(L(\tilde{\eta}_k, u_k, \triangle u_k) + \sum_i \mu_i S_k^i l_k^i + PF_k^{obs} + PF_k^{goal} \Big) \quad (8)$$

where, $i = \triangle u, u, \alpha_f, \alpha_r$ and,

$$\phi(\tilde{\eta}_N) = \frac{1}{2}\tilde{\eta}_N^T P_0 \tilde{\eta}_N \quad (9)$$

$$L(\tilde{\eta}_k, u_k, \triangle u_k) = \frac{1}{2}\tilde{\eta}_k^T Q \tilde{\eta}_k + \frac{1}{2}\triangle u_k^T R \triangle u_k + \frac{1}{2} u_k^T T u_k \quad (10)$$

$$\sum_i \mu_i S_k^i l_k^i = \mu_u S_k^u l_k^u + \mu_{\triangle u} S_k^{\triangle u} l_k^{\triangle u} + \mu_\alpha S_k^{\alpha_f} l_k^{\alpha_f} + \mu_\alpha S_k^{\alpha_r} l_k^{\alpha_r} \quad (11)$$

where N is the horizon-length. η_k, $\tilde{\eta}_k$ and $\triangle u_k$ are formulated as $\eta_k = C\xi_k$, $\tilde{\eta}_k = \eta_{k,ref} - \eta_k$, $\triangle u_k = u_k - u_{k-1}$ and μ_i $(i = \triangle u,\ u,\ \alpha_f,\ \alpha_r)$ are KKT variables. P_0, Q, R, T are weighting parameters. The fourth and fifth terms of (8) are potential-like functions to guide the UGV into the destination avoiding obstacles. The potential-like function for obstacles avoidance is constructed with consideration of the polygonal UGVs. We constructed that potential-like function with two different approach. The first one is based on the distance between the vehicle and the obstacles. And the second one is based on the parallax information of the vehicle about the obstacles. Details about these approaches will be given in Sec. 3.2. The following equation is the potential-like function to guide the UGV toward the target point.

$$PF_k^{goal} = K_{goal} \cdot ||q_k - q_{goal}||^2 \quad (12)$$

q_k, q_{goal} are XY coordinate of the center of gravity of the robot and location of the destination in the inertial frame. Equation (9) penalizes the deviation at the final stage. The first term of (10) is the penalty on the deviation from the desired trajectory. The second term penalizes the large control signal difference. And the last term is for the sake of driving in a straight line rather than a curve line. Equation (11) contains penalty on the larger values than the fixed saturation values, defined as the following.

$$S_k^{\triangle u} = |\triangle u_k| - \triangle u_{sat} \quad S_k^u = |u_k| - u_{sat}$$
$$S_k^{\alpha_f} = |\alpha_{f,k}| - \alpha_{sat} \quad S_k^{\alpha_r} = |\alpha_{r,k}| - \alpha_{sat} \quad (13)$$

$$l_k^i = \begin{cases} 0 & , \text{ if } S_k^i < 0\ , \\ 1 & , \text{ else }. \end{cases} \quad (14)$$

where i : $\triangle u,\ u,\ \alpha_f,\ \alpha_r$. These terms are formulated as constraints in the model predictive framework. KKT variables mean the weights of the penalty about constraint violation of the state variables and steering input. Since there exists a trade-off in choosing each KKT variable, we assign their values by comparing the order of magnitude of S_k^i $(i = \triangle u, u, \alpha_f, \alpha_r)$. The online optimization was solved using the augmented lagrangian approach(Kim et al [2002]). Fig. 3 shows the architecture of control flow of the UGVs in unknown environment.

3.2 Potential-like function for obstacle avoidance

For obstacles avoidance of the polygonal vehicle, laser scanners are attached in the front, the left side and the right side with limited sensor range as following the Fig. 4(a). We need not detect the rear side of the vehicle because we only control the front steering angle at a high speed, although the proposed approach can be easily generalized for the backward motion.

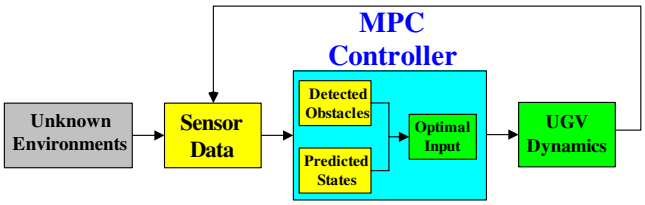

Fig. 3. Architecture of local planner for obstacle avoidance in unknown environment.

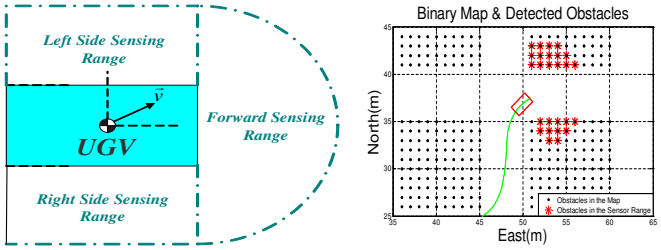

(a) (b)

Fig. 4. (a) The UGV is assumed rectangular. The sensor range can be divided into three regions. (the front, the left side and the right side) (b) The red rectangle is the UGV. The green line is the trajectory of the UGV. The obstacles in the binary map are expressed as black dots. The red dots are the detected obstacles within the fixed sensor range.

Obstacles only within the sensor range are represented as a binary map, and the vehicle has to avoid obstacles with this limited information (see Fig. 4(b)). For constructing the potential-like function to avoid the obstacles, the following two approaches are considered.

1. Approach based on the minimum distance Normally for point mass dynamics, potential-like functions for obstacles avoidance are based on the distance between the UGV and the obstacles. In Kim et al [2002], a potential-like function for successful obstacle avoidance of a rotor-craft based unmanned aerial vehicles(UAVs) is based on the minimum distance between the vehicle and the detected obstacles without considering a speed of the vehicle. If then, there can be a lot of endeavor for tuning weighting parameters, because control becomes harder as the speed of a vehicle increases. As an extension of Kim et al [2002], the following potential-like function based on the minimum distance from obstacles can be constructed.(Yoon et al [2007a], Yoon et al [2007b])

$$PF_k^{obs} = K_{obs} \frac{d_{cf}}{d_{min} + \epsilon}$$
$$d_{min} = ||q_k^{UGV} - q_k^{obs}||_{min} \quad (15)$$
$$d_{cf} = K_{cd} \cdot v$$

where $q_k^{UGV} \in Q^{UGV}$ and $q_k^{obs} \in Q^{obs}$. Q^{UGV} and Q^{obs} are the sets whose elements are the locations of the

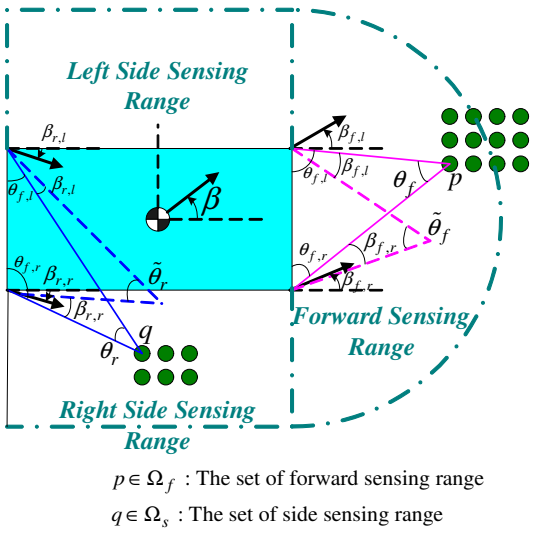

Fig. 5. Modified parallax values corresponding to the dimension, attitude and slip angle of the vehicle

sensor spots around the UGV and the location of the detected obstacle, respectively. d_{cf} is the critical minimum distance that varies with the speed of the vehicle. ϵ is for nonsingularity.

Equation (15) incorporates the speed information, but the UGV in consideration is nonholonomic model. And obstacles located in front are more dangerous than those located in the side of the UGV at the same distance. The approach based on the minimum distance from obstacles cannot reflect this different threat with respect to the location of obstacles. Due to this characteristics of the UGV, optimization process can be difficult and take a long computation time. In the worst case, successful obstacle avoidance may be unsuccessful.

2. Approach based on the parallax information To complement the above drawback, another potential-like function, which is based on the MP for consideration of the dimension of the UGV, is constructed.

Let θ_f and θ_r denote the parallax values from the front sides of the UGV's body to an obstacle in the front sensing range, and from the rear side of the UGV's body to an obstacle in the side sensing range, respectively(see Fig. 5). The four side angles($\theta_{f,l}$, $\theta_{f,r}$, $\theta_{r,l}$ and $\theta_{r,r}$), can be calculated with the geometric consideration:

$$\begin{aligned} \theta_{f,l} &= \tan^{-1}\left(\frac{p_x - \frac{L}{2}}{\frac{w}{2} - p_y}\right), \ \theta_{f,r} = \tan^{-1}\left(\frac{p_x - \frac{L}{2}}{\frac{w}{2} + p_y}\right) \\ \theta_{r,l} &= \tan^{-1}\left(\frac{q_x + \frac{L}{2}}{\frac{w}{2} - q_y}\right), \ \theta_{r,r} = \tan^{-1}\left(\frac{q_x + \frac{L}{2}}{\frac{w}{2} + q_y}\right) \end{aligned} \tag{16}$$

p_x, p_y and q_x, q_y are coordinates of the detected obstacle location with respect to the UGV's frame in forward and side sensing range, respectively. These values reflect the dimension of the vehicle, but not the information of of the sideslip angle of each vertex of the vehicle. So we need to consider the sideslip angles of the all vertices of the vehicle. We modify θ_f and θ_r to $\widetilde{\theta}_f$ and $\widetilde{\theta}_r$, in order to solve this issue for forward and side obstacle avoidance, as explained below.

The sideslip angles of the four vertices($\beta_{f,l}, \beta_{f,r}, \beta_{r,l}, \beta_{r,r}$) and the speeds($v_{f,l}, v_{f,r}, v_{r,l}, v_{r,r}$) satisfy the following relationships:

$$\begin{array}{cc} X-axis & Y-axis \\ v_{f,l}\cos\beta_{f,l} = v\cos\beta - \frac{w}{2}\dot{\psi}, & v_{f,l}\sin\beta_{f,l} = v\sin\beta + \frac{L}{2}\dot{\psi} \\ v_{f,r}\cos\beta_{f,r} = v\cos\beta + \frac{w}{2}\dot{\psi}, & v_{f,r}\sin\beta_{f,r} = v\sin\beta + \frac{L}{2}\dot{\psi} \\ v_{r,l}\cos\beta_{r,l} = v\cos\beta - \frac{w}{2}\dot{\psi}, & v_{r,l}\sin\beta_{r,l} = v\sin\beta - \frac{L}{2}\dot{\psi} \\ v_{r,r}\cos\beta_{r,r} = v\cos\beta + \frac{w}{2}\dot{\psi}, & v_{r,r}\sin\beta_{r,r} = v\sin\beta - \frac{L}{2}\dot{\psi} \end{array}$$

From the above equations, $\beta_{\cdot,\cdot}$ can be obtained as the following function of the v, β, $\dot{\psi}$:

$$\begin{aligned} \beta_{f,l} &= \tan^{-1}\left(\frac{v\sin\beta + \frac{L}{2}\dot{\psi}}{v\cos\beta - \frac{w}{2}\dot{\psi}}\right) \\ \beta_{f,r} &= \tan^{-1}\left(\frac{v\sin\beta + \frac{L}{2}\dot{\psi}}{v\cos\beta + \frac{w}{2}\dot{\psi}}\right) \\ \beta_{r,l} &= \tan^{-1}\left(\frac{v\sin\beta - \frac{L}{2}\dot{\psi}}{v\cos\beta - \frac{w}{2}\dot{\psi}}\right) \\ \beta_{r,r} &= \tan^{-1}\left(\frac{v\sin\beta - \frac{L}{2}\dot{\psi}}{v\cos\beta + \frac{w}{2}\dot{\psi}}\right) \end{aligned} \tag{17}$$

And p_x, p_y, q_x, q_y are functions of ψ, X, Y as the following:

$$\begin{bmatrix} P_x \\ P_y \\ 1 \end{bmatrix} = \begin{bmatrix} \cos\psi & -\sin\psi & X \\ \sin\psi & \cos\psi & Y \\ 0 & 0 & 1 \end{bmatrix} \begin{bmatrix} p_x \\ p_y \\ 1 \end{bmatrix} \tag{18}$$

where P_x, P_y and Q_x, Q_y are coordinates of obstacles with respect to the inertial frame. X and Y are location of the center of gravity of the vehicle in the inertial frame. Then p_x, p_y, p_x, p_y will be,

$$\begin{aligned} p_x &= (P_x - X)\cos\psi + (P_y - Y)\sin\psi \\ p_y &= (P_y - Y)\cos\psi + (-P_x + X)\sin\psi \\ q_x &= (Q_x - X)\cos\psi + (Q_y - Y)\sin\psi \\ q_y &= (Q_y - Y)\cos\psi + (-Q_x + X)\sin\psi \end{aligned} \tag{19}$$

Using the above (16) and (18), the modified parallax values $\widetilde{\theta}_f$ and $\widetilde{\theta}_f$ are defined as the following:

$$\begin{aligned} \widetilde{\theta}_f &= \pi - [(\theta_{f,l} - \beta_{f,l}) + (\theta_{f,r} + \beta_{f,r})] \\ \widetilde{\theta}_r &= \pi - [(\theta_{r,l} - \beta_{r,l}) + (\theta_{r,r} + \beta_{r,r})] \end{aligned} \tag{20}$$

To avoid the obstacles safely, these MP values need to be small. Now, let p and q represent the location of the obstacles with the largest MP among the detected obstacles within the forward and side sensing range, respectively, represented in the vehicle's coordinate frame. Then the potential-like function at step k is defined as the following:

$$PF_k^{obs} = \begin{cases} 0 & \text{nothing,} \\ K_{obs} \exp\left(\dfrac{\widetilde{\theta}_f}{\theta_{cf}(v)}\right) & p \text{ exists,} \\ K_{obs} \exp\left(\dfrac{\widetilde{\theta}_r}{\theta_{cr}(v)}\right) & q \text{ exists,} \\ K_{obs} \exp\left(\dfrac{\widetilde{\theta}_f}{\theta_{cf}(v)} + \dfrac{\widetilde{\theta}_r}{\theta_{cr}(v)}\right) & p,\ q \text{ exist.} \end{cases} \quad (21)$$

$\theta_{cf}(v)$ and $\theta_{cr}(v)$ are the critical MP values which are the function of v. They have to be decreased as the speed of the UGV increases, so we define them as

$$\theta_{cf} = \frac{K_{cf}}{v}, \quad \theta_{cr} = \frac{K_{cr}}{v}$$

4. SIMULATION RESULTS

To validate the performance of the suggested approach for obstacles avoidance, simulations were performed. An UGV is supposed to follow the straight line connecting the known start and the goal points with the initial speed of 4 m/s. But on the way to the destination, the UGV notices the obstacles and replans to avoid them. Initially the UGV was located at [5 m, 5 m] in the inertial coordinate frame while heading east. To compare the two approaches described in Sec. 3.2, two scenarios are tested. The first scenario is navigation in a simple area composed of two circular obstacles. And in the second scenario, an urban area which is composed of many structures and narrow lanes was assumed. The sensor range was assumed 5 m, and the following parameters were used.

horizon length(N)	15
sample time ($\triangle t$)	0.05 sec
steering angles	$-30\ ^\circ \leq \delta_f \leq 30\ ^\circ$
changes of steering angles	$-3\ ^\circ \leq \Delta\delta_f \leq 3\ ^\circ$
slip angle of a tire	$-4\ ^\circ \leq \alpha. \leq 4\ ^\circ$

4.1 Circular obstacles

In this scenario, the environment contains two circular obstacles.

In Fig. 6 (a)-(g), the blue curve is the result from using MP, and the red is the result from using distance from the obstacles. As can be seen in Fig. 6(a) performances in terms of collision-free navigation are satisfactory in both cases. In Fig. 6 (b), (f), (g), the black dotted lines are the saturation values for the corresponding variables and the plots show those variables are kept within the saturation values.

Approach	t_r	t_{cpu}	γ_{mean}
MP	33.55 sec	17.2640 sec	1.6613 m
Distance	33.60 sec	124.2945 sec	1.4624 m

From Fig. 6 it seems that there exists no clear difference between the two approaches. But in the view of the computational efficiency, the approach based on the MP was better. From the above table, the time(t_r) until the UGV arrives at its own target point is similar, but computation time(t_{cpu}) contrasts sharply about seven times. γ_{mean} is the mean deviation from the reference path.

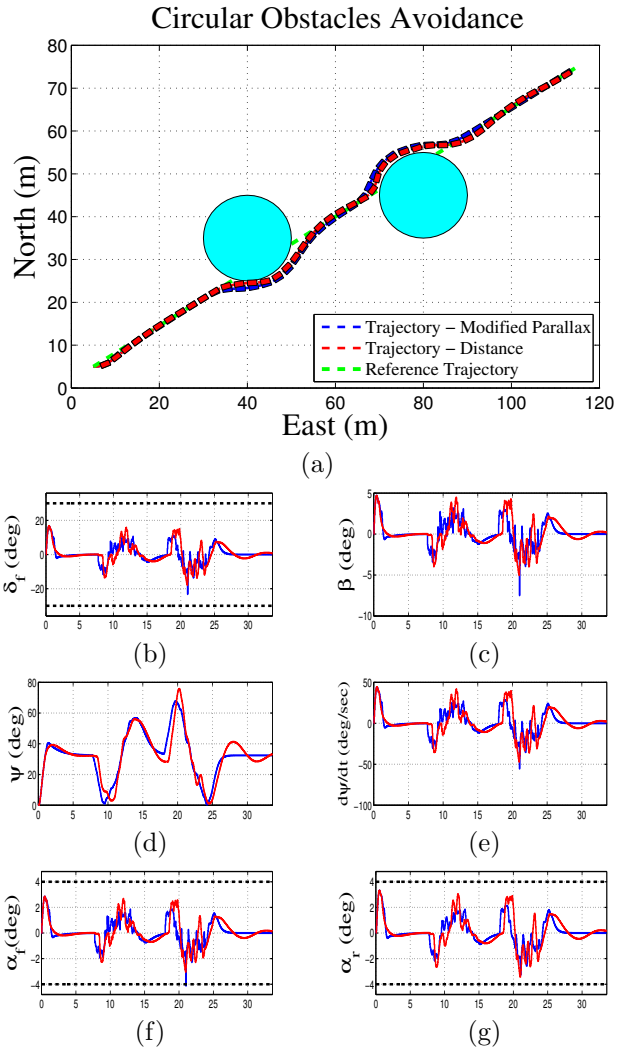

Fig. 6. (a) The trajectories of the UGVs. (b) steering angle commands. (c) sideslip angles of the UGVs. (d) heading angles. (e) rate of the heading angles. (f) slip angles of the front wheel. (g) slip angles of the rear wheel. In each plot, the blue is from the approach based on the MP, and the red is from the approach based on the distance.

4.2 Urban environment

In this scenario, UGV is supposed to navigate in the urban area. In this area, many rectangular structures exist. Polygonal obstacles are often more difficult to avoid than circular obstacles due to their sharp edges while tracking the given reference.

As can be seen in Fig. 7(a), only the approach based on the MP avoided the obstacles successfully. As mentioned in Sec. 3.2, in a complex area, with the information of distance from obstacles only it is not easy to pick out the most dangerous obstacle. Moreover, the most dangerous obstacle can change with respect to the heading of the UGV. If the approach based on the pure MP of the UGV is applied, the heading of the UGV cannot be considered. Since we modified the MP using the heading of the UGV, the most dangerous obstacle can be picked out efficiently.

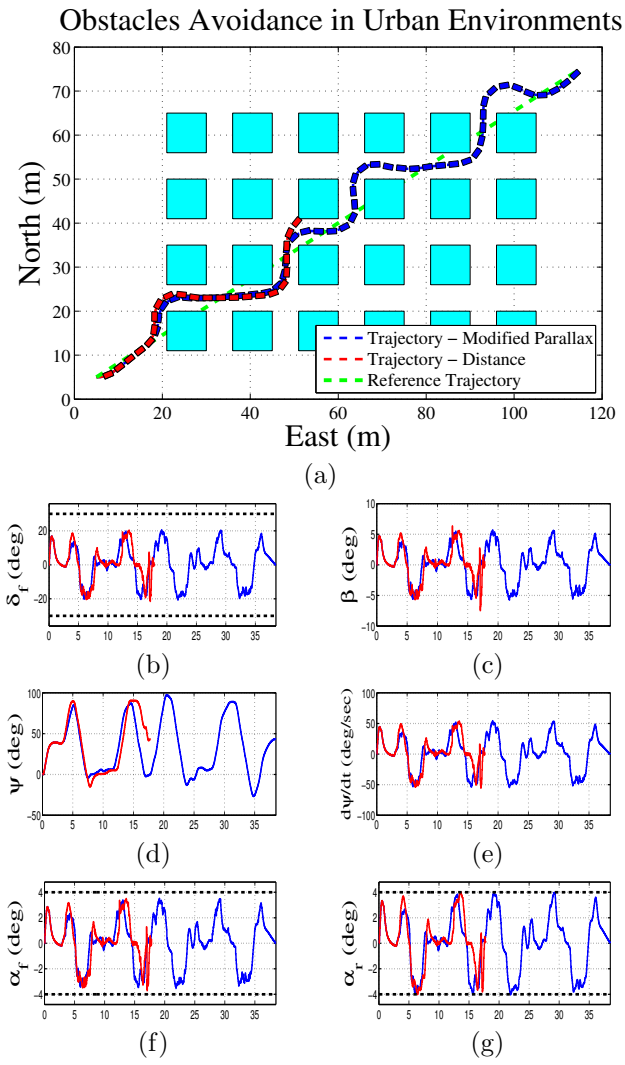

Fig. 7. (a) The trajectories of the UGVs. (b) steering angle commands. (c) sideslip angles of the UGVs. (d) heading angles. (e) rate of heading angles. (f) slip angles of the front wheel. (g) slip angles of the rear wheel. In each plot, the blue is from the approach based on the modified MP, and the red is from the approach based on the distance.

Approach	t_r	t_{cpu}	γ_{mean}
MP	38.50 sec	17.9411 sec	3.1103 m
Distance	(17.25 sec)	214.9126 sec	3.3717 m

The above table shows superiority of the approach based on the modified MP. t_r of (17.25 sec) means that the minimum-distance approach failed after 17.25 sec. On the other hand, the maximum-MP approach successfully finished the navigation about twice faster than the real time.

5. CONCLUSION

A model predictive approach for obstacles avoidance of a car-like robot was presented. An optimal problem while avoiding obstacles was formulated in terms of cost minimization under constraints. We solved this with nonlinear programming and the constraints were incorporated as a penalty function with KKT variables. For obstacles avoidance with consideration of the dimension of the UGV, two kinds of potential-like functions are proposed. The first one is based on the minimum distance from the obstacle. And the other is based on the MP considered with the dimension and the heading of the UGV. Simulation results show that the approach with the modified MP is superior especially in a complex environment. By incorporating both the velocity and heading information of the UGV, the proposed approach can efficiently avoid the collision.

REFERENCES

E. Rimon, D. Kodischek. Exact robot navigation using artificial potential functions. *IEEE Transaction on Robotics and Automation*, 8(5):501–518, 1992.

D. Fox, W. Burgard and S. Thrun. The dynamic window approach to collision avoidance. *IEEE Robotics and Automation Magazine 4(1)*, 23–33, 1997.

R. G. Simmon. The curvature velocity method for local obstacle avoidance. *IEEE International Conference on Robotics and Automation*, vol 4, 2275–2282, 1996.

J. Minguez and L. Montano. Nearness diagram navigation(ND): a new real-time collision avoidance approach. *IEEE/RSJ International Conference on Intelligent Robots and System(IROS)*, 2000.

I. Ulrich and J. Borenstein. VFH: Reliable obstacle avoidance for fast mobile robots. *IEEE International Conference on Robotics and Automation*, pp.1572–1577, 2000.

K. O. Arras, J. Persson, N. Tomatis, R. Siegwart. Real-time obstacle avoidance for polygonal robots with a reduced dynamic window. *IEEE International Conference on Robotics and Automation*, Washington, DC., May 2002.

E. Bakker, L. Nyborg and H. B. Pacejka. Tyre modeling for use in vehicle dynamics studies. *SAE paper*, ♯ 870421, 1987.

D. Wollherr. Robust steering control for swerving manoeuvres of a motor vehicle. PhD thesis, Automotic Control Lab, ETH, Zurich, 2002.

F. Borrelli, P. Falcone, T. Keviczky, J. Asgari and D. Hrovat. MPC-based approach to active steering for autonomous vehicle systems. *International Journal of Vehicle Autonomous Systems*, **3**(2/3/4), 265–291, 2005.

P. Falcone, F. Borrelli, J. Asgari, H. E. Tseng and D. Hrovat. Predictive active steering control for autonomous vehicle systems. *IEEE Transactions on Control Systems Technology*, 2007.

H. J. Kim, D. H. Shim and S. Sastry. Nonlinear model predictive tracking control for rotorcraft-based unmanned aerial vehicles. *American Control Conference*, Anchorage, AK, pp 3576–3581, May 2002.

Yongsoon Yoon, H. Jin Kim, Tokson Choe and Yongwoon Park. Safe steering of UGVs in polygonal environments. *International Conference on Control, Automation and Systems*, Seoul, October, 2007.

Yongsoon Yoon, H. Jin Kim, Tokson Choe and Yongwoon Park. Communication in distributed model predictive collision avoidance. *International Conference on Robot Communication and Coordination*, Athens, October, 2007.